Standalone Photovoltaic Water Pumping System Using Induction Motor Drive with Reduced Sensors

Bhim Singh, *Fellow, IEEE*, Utkarsh Sharma, *Member*, *IEEE*, and Shailendra Kumar, *Member*, *IEEE*

***Abstract* - A simple and efficient solar photovoltaic (PV) water pumping system utilizing an induction motor drive (IMD) is presented in this paper. This solar PV water pumping system comprises of two stages of power conversion. The first stage extracts the maximum power from a solar PV array by controlling the duty ratio of a DC-DC boost converter. The DC bus voltage is maintained by the controlling the motor speed. This regulation helps in reduction of motor losses because of reduction in motor currents at higher voltage for same power injection. To control the duty ratio, an incremental conductance (INC) based maximum power point tracking (MPPT) control technique is utilized. A scalar controlled voltage source inverter (VSI) serves the purpose of operating an IMD. The stator frequency reference of IMD is generated by the proposed control scheme. The proposed system is modeled and its performance is simulated in detail. The scalar control eliminates the requirement of speed sensor/encoder. Precisely, the need of motor current sensor is also eliminated. Moreover, the dynamics are improved by an additional speed feedforward term in the control scheme. The proposed control scheme makes the system inherently immune to the pump's constant variation. The prototype of PV powered IMD emulating the pump characteristics, is developed in the laboratory to examine the performance under different operating conditions.**

***Index terms*- Photovoltaic cells, MPPT, water pumping, scalar control, induction motor drives**

I. INTRODUCTION

The rising energy crises throughout the world and pollution of natural habitats, have been seeking attention from engineering and science fraternity since couple of decades. The knowledge for manifestation of renewable energy sources into useful form, has been maturing rapidly. The advent of fast switching power electronic devices and development in semiconductor technology, have majorly contributed to energy conversion methods. The renewable energy utilization, which started from converting the energy of running water, has travelled across to convert solar energy to electrical energy directly today.

Solar photovoltaic (PV) energy converters earlier have been inefficient with the efficiency as low as 5-6 % and highly costly [1]. However, with increased technological research and advancements, the efficiency of PV array, at present, has reached 15-16%. Moreover, the prices have been reducing gradually. Today, PV energy conversion is viewed as one of the promising alternatives to fossil fuel based electricity generating systems, as there are no toxic emissions, no greenhouse gases emission, no fuel cost involvement, least maintenance cost, no water use etc. However, the technology is in developing phase and there are many challenges which need to be addressed such as, intermittency, high initial cost and low efficiency.

Manuscript received on 6-July-2017, revised on 19-September-2017 and 4-January-2017 and accepted on 12-March-2018. This work was supported by DST, Govt. of India (RP03128G, RP02926 and RP03222G)

B. Singh, U. Sharma and S. Kumar are with Department of Electrical Engineering, Indian Institute of Technology Delhi, New Delhi, India.
E-mail: utkarsh.kota@gmail.com

The solar water pumps [2]-[4] are gaining the popularity in rural areas, where the electricity is not available. Moreover, solar PV fed water pumps are the favored in remote areas for irrigation, water treatment plant, and agriculture purpose. Country like India, where 70% population depends upon agriculture, therefore, irrigation is necessary for good yield. There is large number of water pumps in the world running with electricity or with non-renewable energy sources. The acquisitions of solar PV based water pumping systems [5] are more convenient as compared to diesel based water pumping systems in respect to the cost and pollution.

The design of a motor drive system powered directly from a PV source, demands creative solutions to face the challenge of operation under variable power restrictions and still maximize the energy produced and the amount of water pumped [6].

In PV pumping (PVP) systems, an induction motor drive (IMD) shows good performance as compared to other commercial motors because of its rugged construction. The evolution is intended to develop productive, reliable, maintenance-free and cheap PV water pumping system [7]. However, new permanent magnet motors such as brushless DC motor and permanent magnet sine fed motors are used into pumping, but are still overshadowed by induction motor because of cost and availability constraints [8]. Moreover, the manufacturing of the induction motor is in matured stage giving an edge to its use in developing countries for solar water pumping application. With the emergence of outperforming solid state switches, high speed processors and efficient motor control algorithms, IMD based water pumping systems have taken a step ahead to conventional water pumping systems. Moreover, PV array fed IMD has performed ruggedly in the field of pumping system by utilizing a VSI (Voltage Source Inverter). The proposed work deals with a three-phase IMD for solar water pumping, which meets the requirement of life without electricity in remote locations.

The initial cost of solar power plant is high. Therefore, once the plant is installed, the focus is to obtain the peak power from the solar panels of the installed capacity. The developed water pumping system powered directly from PV array, requires MPPT algorithms to operate under different irradiation levels and to extract the peak power from a solar PV array. Some of these, MPPT algorithms are recommended in [9]. A comparative study on different MPPT techniques is provided in [10]-[12]. From operational point of view, MPPT is a mandatory segment of a PV system. The substantial research is reported in past few years in the area of MPPT. In this paper, an INC (Incremental Conductance) based technique is used to obtain the peak power from the solar PV array. Therefore, the proposed PV fed water pumping system produces peak torque even at low radiation. The INC technique is based on the comparison of output conductance of solar PV array to the incremental conductance. As compared to solar PV grid interfaced systems [13], the major challenge in PV water pumping is

This article has been accepted for publication in a future issue of this journal, but has not been fully edited. Content may change prior to final publication. Citation information: DOI 10.1109/TIA.2018.2825285, IEEE Transactions on Industry Applications

timely control of active power. This is due to the fact that the mechanical time constant of the motor pump system is much higher than that of aforementioned system. Under sudden fall in solar insolation, the PV array voltage tends to reduce drastically and consequently the level of flux in the motor falls rapidly. Once the flux has been fallen, the motor starts drawing higher current, which is limited by the short circuit current of the PV array in order to rebuild the flux. The operating point in the I vs V curves of PV array, shifts to current source region demonstrated by short circuit current and very low voltage. Due to insufficient power, the motor starts operating in an unstable zone of torque-speed characteristics near to a point where slip = 1. This particular condition is menacing for the motor health and once the motor enters this zone then there has to be a provision in the control, which can identify this condition and restart the motor from the standstill condition. The motor entering into such situations frequently, would reduce the overall duty of the pump, hence it's the responsibility of MPPT algorithm to take care of such events.

To control the IMD tied VSI, a simple V/*f* (voltage/ frequency) control approach is utilized in [14], [15]. The pumping system with a DC-DC converter and VSI is used for water pumping application in [16]-[18]. However, presented approach suffers from DC link voltage instability. V/*f* approach is simple, easy to implement and cost effective. Dual inverters are used to supply power to centrifugal pump with SAZEPWM technique [19]. Apart from V/*f* control, DTC (Direct Torque Control) and vector control techniques are complicated and they require extra current sensors for implementation [20]. In V/*f* control, only PV array current, voltage, and DC bus voltage are sensed. The proposed system tracks the MPP point by altering the modulation frequency so that the IMD is able to extract the maximum power from the solar PV array at sustained torque for different solar insolation levels. The proposed system is able to supply more water as compared to a solar PV fed DC motor based water pump. By utilizing V/*f* control, the starting performance of the IMD is improved even if IMD is started with lower solar insolation. Therefore, water is permanently pumped from morning to till the evening. The starting current of the induction motor connected to the fixed voltage AC mains is around 5 to 6 times of full load current. Therefore, to start the motor without any control, higher numbers of solar modules are required. Whereas, smooth starting of the induction motor is possible by using V/*f* control without drawing high starting current. This also improves the life of the motor. Moreover, the areas which are blessed with the electrical connectivity, may utilize the grid interfaced PVPs [21]. In Indian context, still many indoor villages and agricultural lands do not possess a privilege of having electrical network.

II. DESIGN OF PROPOSED SYSTEM

The system configuration for PV water pumping system is depicted in Fig. 1. It consists of a PV array followed by a boost converter. A VSI is used to provide pulse width modulated voltage input to the motor and pump assembly. The power from a PV array is regulated using an incremental conductance method to attain its maximum value with available radiation. The V/*f* control is used to give reference speed to IMD.

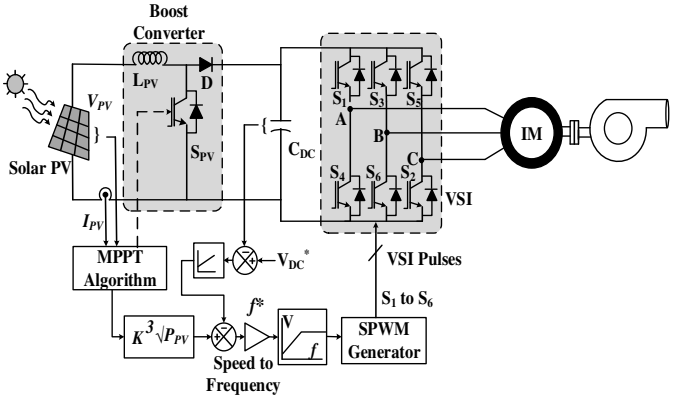

Fig. 1. System architechure for the standalone solar water pumping system

A. Design of Solar PV Array

An induction motor of a 2.2 kW is selected for proposed system. If losses of the motor and pump are neglected, the capacity of the PV array should be equivalent to the motor capacity. In this case, a PV array is selected as of 2.4 kW.

$$P_{mp} = \left(N_p \times I_{mp}\right) \times \left(N_s \times V_{mp}\right) = 2.4 \text{ kW} \quad (1)$$

where, P_{mp} is the maximum power that can be drawn from panels at a given radiation, V_{mp} is the PV panel voltage at MPP and I_{mp} is the current at MPP. N_s and N_p are the number of modules connected in series and parallel, respectively. Considering an open circuit voltage of the panel to be near to a DC link voltage and power drawn from a panel to be 2.4 kW, number of modules in series and parallel are selected to be 11 and 1. The individual module and array specifications are provided in Table I.

TABLE I
SPECIFICATIONS OF THE SOLAR MODULE AND ARRAY

Module peak power of the single module	225 W
Module open circuit voltage (v_{oc})	41.79 V
Module short circuit current (i_{sc})	7.13 A
Module voltage at MPP (v_{mp})	33.9 V
Module current at MPP (i_{mp})	6.63 A
Array peak power (P_{mp})	2.4 kW
Array open circuit voltage (V_{oc})	459.69
Array short circuit current (I_{sc})	7.13 A
Array voltage at MPP (V_{mp})	372.9 V
Array current at MPP (I_{mp})	6.63 A

B. Selection of DC Link Voltage

The DC bus voltage of VSI is estimated from a relation as,

$$m \times \frac{V_{DC}}{2\sqrt{2}} = \frac{V_{L-L}}{\sqrt{3}} \quad (2)$$

where, m is the modulation index and $V_{L\text{-}L}$ is a line voltage across the motor terminals. Hence,

$V_{DC} = \frac{2\sqrt{2}}{\sqrt{3}} \times 230 = 375V$, the voltage which is required when modulation index is 1. The DC link voltage is chosen to 400 V.

C. Design of DC Link Capacitor

The DC link capacitor is supposed to provide sufficient energy at the time of transients such as fall in radiation and an increase in the load. Its value is calculated as [22],

$$\frac{1}{2} C_{DC} [V^{*2}_{DC} - V^2_{DC1}] = 3\alpha VIt \quad (3)$$

$$\frac{1}{2} C_{DC} [400^2 - 375^2] = 3 \times 1.2 \times 133 \times 8.2 \times 0.005$$

C_{DC} = 2026 μF

In above expression, V_{DC}^* refers to the set DC bus voltage while V_{DC1} is acceptable lower most voltage during transients. Morever, α is an overloading factor and t is duration of transient.

D. Selection of DC-DC Boost Converter

The boost inductor duty cycle, D is given as [23],

$$D = \frac{V_{DC} - V_{mp}}{V_{DC}} = \frac{400 - 373}{400} = 0.0675 \tag{4}$$

$$L_m = \frac{V_{mp} D}{\Delta I_1 f_s} = \frac{372.9 \times 0.0677}{(0.2 \times 7.6 \times 10000)} = 1.875\ mH \tag{5}$$

Thus the inductance L value is selected as 3 *m*H.

where, f_s is switching frequency, ΔI_1 is amount of ripple current.

E. Design of Pump

For a selected water pump, proportionality constant (K_{pump}) is given as,

$$K_{pump} = \frac{T_L}{\omega_r^2} \tag{6}$$

where, T_L is the load toque of water pump, which is equal to the torque offered by an induction motor under steady state operation and ω_r is the rotational speed of the rotor in rad/sec. Since the rated torque and rated speed of the induction motor are 14.69 N-m and 1430 rpm. Then proportionality constant (K_{pump}) is estimated using (6) as,

$$K_{pump} = \frac{14.69}{(2 * \pi * 1430/60)^2} = 6.55 \times 10^{-4}\ N - m/(\text{r ad/s})^2$$

So proportionality constant is selected as $6.55*10^{-4}$ N-m/(r/s)^2.

III. Control Scheme for Proposed System

The proposed topology is a two stage power conversion system for a solar PV array fed water pumping. It embodies scalar control for IMD operation and an incremental conductance (INC) method for maximum power extraction from the PV array. The simplicity and ease of implementation of scalar control overshadows precise but computation intensive control algorithms such as vector control and direct torque control. Moreover, in later mentioned algorithms, the sensorless operation is itself an exhaustive task. The voltage and current of PV array are sensed and fed to the INC algorithm. Based on the change in voltage, current and power, this algorithm decides the duty ratio of the boost converter. The boost converter output voltage is maintained to a constant value using a proportional-integral (PI) controller. Since the pump characteristics are centrifugal in nature, the power absorbed and the speed of the pump have direct relation as mentioned in (6). A speed feed forward term is calculated from the available PV power from which, the PI controller output is subtracted. This is helpful in reducing the burden on the PI controller and improving the dynamic performance of the system. V/*f* control algorithm generates the switching logic for VSI using sinusoidal pulse width modulation. If DC link voltage is higher than the reference value, the PI controller increases the reference speed given to V/*f* control and vice versa. The sum of two quantities gives a resultant speed reference f^* for IMD, which is fed to V/*f* control algorithm. The DC link voltage error is estimated as,

$$V_{DCr} = V_{DC}^* - V_{DC} \tag{7}$$

The output of the DC link voltage PI controller is as,

$$\omega_{DCr(n)} = \omega_{DCr(n-1)} + k_p\{V_{DCr(n)} - V_{DCr(n-1)}\} + k_i V_{DCr(n)} \tag{8}$$

The speed term corresponding to PV power is as,

$$\omega_P = K\sqrt[3]{P_{PV}} \tag{9}$$

where, constant K is derived from pump's constant. The reference frequency of the IMD is as,

$$f^* = \frac{1}{2\pi}\left(\omega_p - \omega_{DCr}\right) \tag{10}$$

Initially the boost converter pulses are kept off such that the system works as a single stage system and the speed is ramped up to a threshold speed. After threshold speed, the control of the boost converter is activated and the duty ratio is calculated from INC algorithm. This is realized to avoid high current at starting since MPPT algorithm gives maximum power even at starting. Using ramp frequency start, the starting current of the motor is limited, which in case of direct online starting (DOL) at rated frequency is about 5-6 times the rated current. Moreover, it prevents the solar PV array to go into current source region at starting as the current drawn is very high in DOL starting.

A. Incremental Conductance Method for MPPT

Solar PV array has nonlinear bell shaped P_{PV} versus V_{PV} characteristics as shown in Fig. 2. At any moment, the operating point depends on the impedance of the load connected to the array terminals. A DC-DC converter is used to track the point of operation on the PV curve. There have been many algorithms in the literature for tracking of maximum power point. Most basic of all, is perturb and observe algorithm, which involves step change in the reference voltage or duty ratio to the DC-DC converter and monitoring of the power output. It faces several issues while radiation changes. An incremental conductance method works much better in dynamic changes in solar insolation. This is due to a fact mentioned in section I, that the mechanical time constant of the motor is much higher than the electrical time constant of the whole system. Proposed work uses an incremental conductance algorithm, which is based on the monitoring of slope of P_{PV} versus V_{PV} curve.

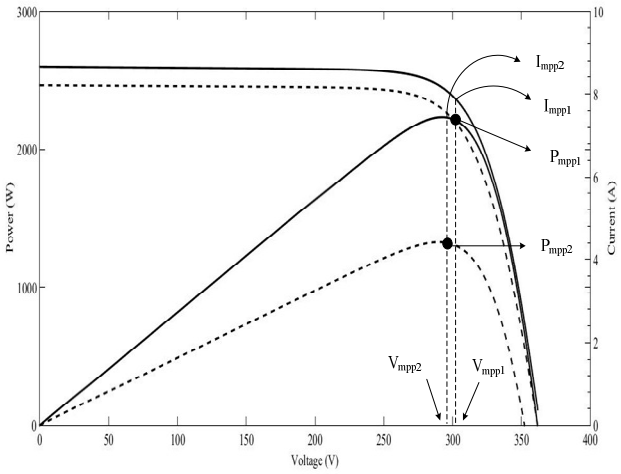

Fig. 2. P vs V and I vs V characteristics of the SPV array

On the right hand side of the MPP, the slope is negative while on the left hand side the slope is positive. At the point, where maximum power is being transferred from the array, the slope of the curve is zero. With change in radiation, at MPP I_{PV} changes drastically, whereas V_{PV} remains constant. Considering a power equation and differentiating it with respect to voltage, relations between an incremental conductance and conductance are obtained for different sections of the curve as,

$$P_{PV} = V_{PV} \times I_{PV} \tag{11}$$

$$\frac{dP_{PV}}{dV_{PV}} = I_{PV} + V_{PV} * \frac{dI_{PV}}{dV_{PV}} = 0 \tag{12}$$

$$\frac{dI_{PV}}{dV_{PV}} = -\frac{I_{PV}}{V_{PV}} \tag{13}$$

on the right side of MPP, slope is negative, which suggests that $\frac{dI_{PV}}{dV_{PV}} < -\frac{I_{PV}}{V_{PV}}$ and on the left side slope is positive meaning $\frac{dI_{PV}}{dV_{PV}} > -\frac{I_{PV}}{V_{PV}}$. At MPP slope is zero means that $\frac{dI_{PV}}{dV_{PV}} = -\frac{I_{PV}}{V_{PV}}$. The duty ratio of the boost converter is adjusted in accordance with the algorithm as shown in Fig. 3.

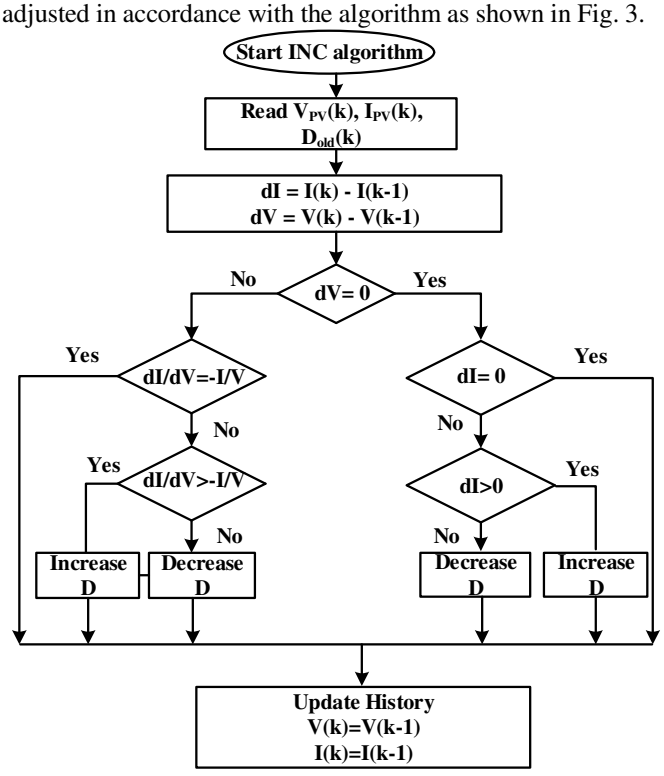

Fig. 3. Flowchart for incremental conductance algorithm for MPPT

B. Scalar (V/f) Control of Induction Motor

The scalar control of an induction motor is most common and simplest control so far. Usually induction motors are designed for 50 Hz input voltage. For the operation at lower speed, the voltage has to be reduced. The frequency control along with voltage magnitude control is also desired for constant flux operation. The voltage should be proportional to the frequency such that flux magnitude is maintained constant as $\psi_s = V/\omega$. An IM is usually fed from a three phase PWM VSI. Only an input parameter is the reference speed. Neglecting the small slip speed, the speed of the motor is approximately equal to the reference speed. The speed reference is integrated to generate the θ, which is used to obtain three sinusoidal voltage references, which are compared with high frequency triangular wave to generate the switching pulses for VSI. The speed reference is estimated from the control scheme as mentioned in previous subsection.

$$\theta = \int \omega^* dt \tag{14}$$

Three phase reference voltages are as,

$$V_a^* = m \times \sin(\theta) \tag{15}$$

$$V_b^* = m \times \sin(\theta - 120°) \tag{16}$$

$$V_c^* = m \times \sin(\theta - 240°) \tag{17}$$

where, $m = k_f \omega^*$, m is the modulation index.

IV. Results and Discussion

Performance of a double stage PV fed water pumping system is evaluated using the simulation package. The proposed system is designed, modelled and simulated in the MATLAB/Simulink environment. The step change in the solar radiation is also simulated in order to determine the satisfactory performance of the system under dynamic conditions.

A. Starting Performance of Proposed System

Fig. 4 exhibits various parameters of the proposed water pumping system at 500 W/m^2 radiation. The DC link of VSI is energized initially. Since the switching device of the boost converter is off, the voltage across the DC link of VSI is the open circuit voltage of PV array. It starts falling once the motor speed increases. The PV array current starts from zero and rises up to I_{mp}. The PV voltage reaches V_{mp} once a threshold frequency is passed and the control of the boost converter is activated for MPPT. At t = 8 s, the boost converter is activated and the system reaches corresponding MPP. The DC link voltage is settled at reference value because of action of PI controller. It is verified from the figure that the motor current never exceeds the rated current, which is by the virtue of soft start. This practice improves the lifespan of the motor.

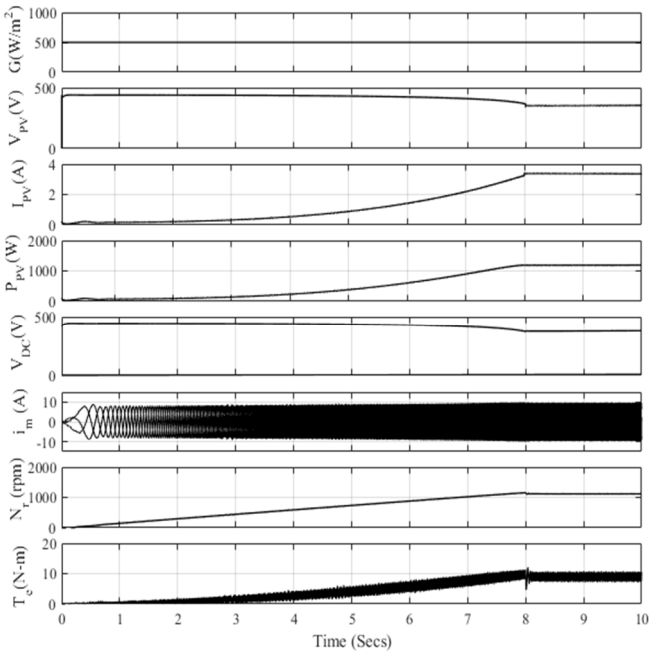

Fig. 4. Starting performance of the proposed system

B. Steady State and Dynamic Performances of Proposed System

The behavior of the proposed standalone PV water pumping system is depicted in Fig. 5. This figure comprises simulation of varied solar insolation changes. From t = 1 s to 2 s, the solar insolation is constant at 800 W/m^2. The PV indices are at the corresponding MPP. At t = 2 s, a slope decrement in the solar insolation is simulated to test the MPPT algorithm effectiveness. The PV voltage observes negligible change while the PV current varies proportional to the available insolation. Moreover, the DC bus voltage is also maintained at reference voltage of 400 V without any failure. The speed and torque of the motor are reduced with the reduction in PV power. This continues to happen till t = 4 s, from where the system experiences a slope increase in the solar insolation. Similar to the previous behavior, the PV current starts increasing proportional to the solar radiation, while there is not much change in the PV voltage. Consequently, the available power from a PV source ramps up along with the motor speed and the motor torque. From t = 6 s, the system operates in steady state at a solar radiation of 1000 W/m^2. The system faces a step decrement in the solar insolation from 1000 W/m^2 to 500 W/m^2 at t = 7 s, owing to which the PV current reduces instantly. However, still the PV voltage does not face much transients. The DC bus voltage experiences slight transient change, however, it restores to a reference voltage quickly. It is noteworthy that, the DC bus voltage is maintained even at 50 % reduction in rated power. Similarly, a step increase in a solar insolation is observed at t = 9 s. As anticipated from previous behavior of the system, the DC bus voltage is maintained to a reference value while there is no significant change in the PV voltage. The motor speed and torque increase proportionally to balance a power from a source.

V. EXPERIMENTAL VALIDATION OF PROPOSED SYSTEM

For the verification of the proposed configuration and the control of proposed system, a prototype is developed in the laboratory, which consists of solar PV simulator (AMETEK ETS 600×17DPVF), a boost converter, a VSI (Semikron Make), a DSP (dSPACE 1104 real time controller) and a three phase induction motor coupled to a DC generator.

A volumetric pump is realized by loading the three phase IMD using a DC generator. A resistive load is set to extract the rated power from the PV source corresponding to the head of pump. The solar PV array characteristics are designed in the simulator software to provide a maximum power of 2.4 kW with an open circuit voltage of 420 V and short circuit of 7 A. Hall-Effect voltage and current sensors (LV-25P and LA-55P respectively) are used to sense the PV voltage, PV current and DC link voltage. An opto-coupler based isolation is provided between the gate driver pulses from DSP to the VSI. Experimental results are discussed as follows.

A. MPPT Performance of PV Array

Figs.6 (a)-(b) show the execution of MPPT along with PV current versus PV voltage and PV power versus PV voltage characteristics. The small circle denotes the operating point as well as MPPT performance in percentage. It is noticed from the figure that MPPT percentage is near to 100 %. Therefore, at rated condition as well as at varying atmospheric conditions, the pumping system extracts the maximum energy from a PV array.

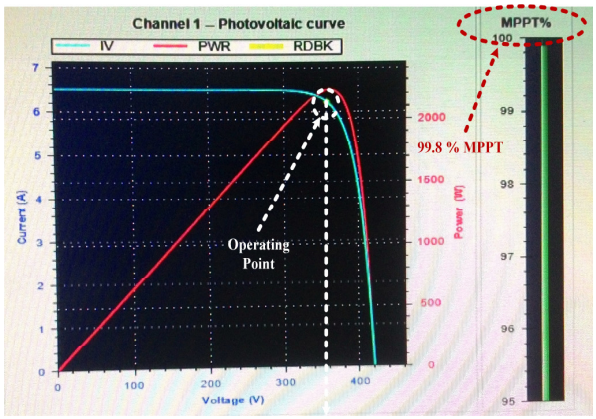

Fig. 6 (a) Performance of the system at 1000 W/m^2 radiation

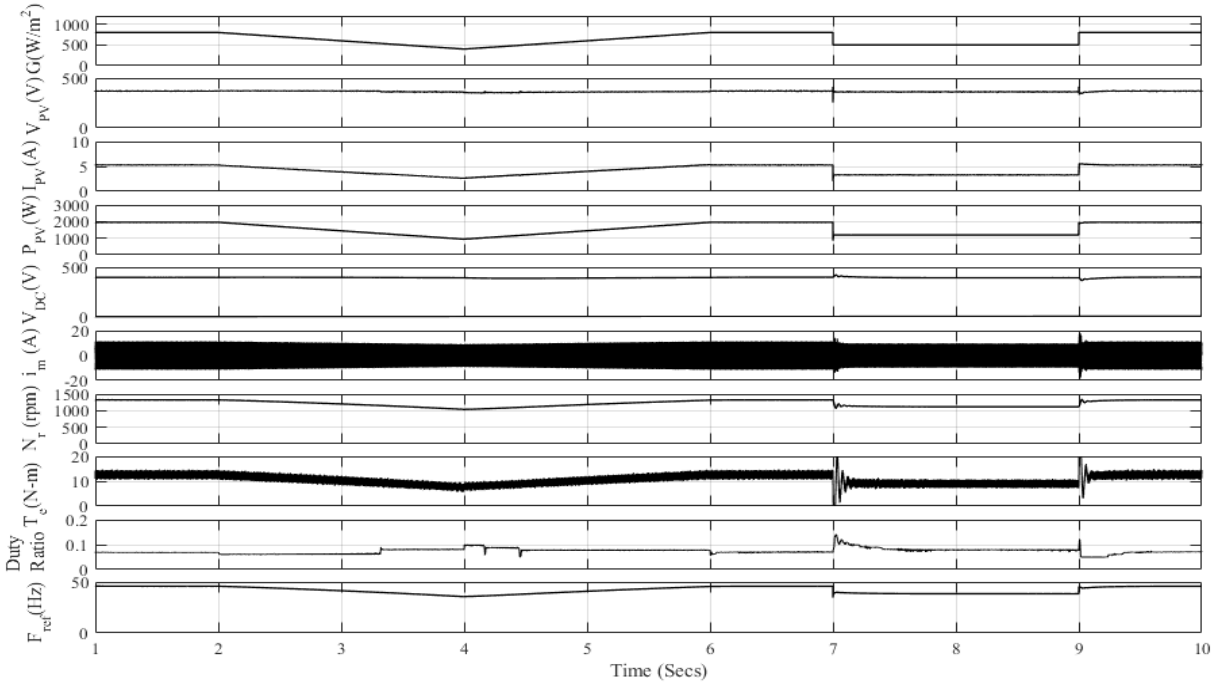

Fig. 5 Steady state and transient behaviour of proposed system

This article has been accepted for publication in a future issue of this journal, but has not been fully edited. Content may change prior to final publication. Citation information: DOI 10.1109/TIA.2018.2825285, IEEE Transactions on Industry Applications

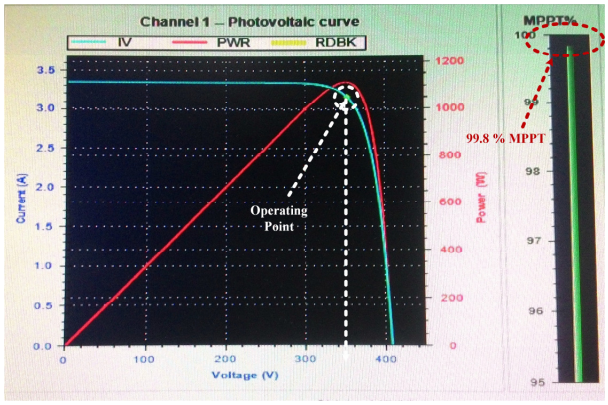

Fig. 6 (b) Performance of the system at 500 W/m^2 radiation

B. *Starting Characterisctics of Proposed System*

Fig. 7 shows a variation in the parameters at starting. Recorded waveforms show DC bus voltage V_{DC}, *PV* current I_{PV}, an IM current i_{ma} and IM speed N_r at 1000 W/m^2 radiation. Initially the boost converter is switched off, MPPT algorithm being dysfunctional. After starting the IMD, the boost converter is switched on at 1200 rpm and the PV array starts operating at MPP. The PV array is found to be operation with the efficiency of more than 99 %.

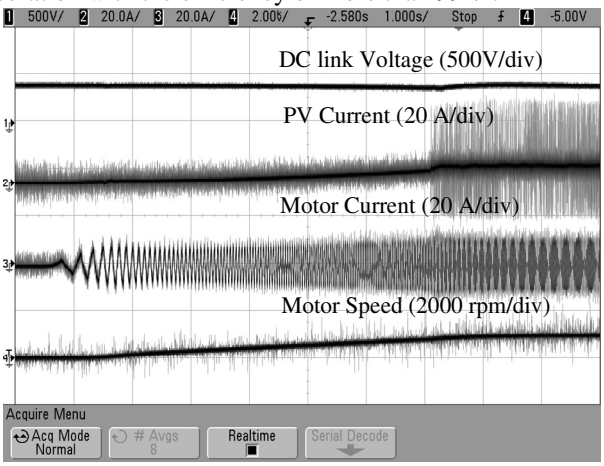

Fig. 7 Experimental characteristics of the system at starting

C. *Steady State Characteristics of Proposed System*

Fig. 8 shows the recorded waveforms of the system under steady state condition. The DC bus voltage V_{DC}, PV current I_{PV}, motor current i_{ma} and motor speed N_r are depicted in the figure.

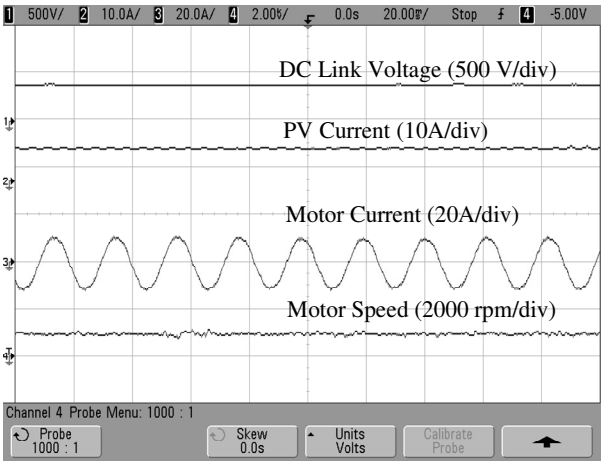

Fig. 8 Steady state response of the system V_{DC}, I_{PV}, i_{ma} and N_r

Fig. 9 shows V_{DC}, D, I_{PV} and N_r. At steady state condition, the duty ratio is found to be 0.12. At this steady state condition, the motor operates at 1330 rpm. The purpose of Fig. 9 is to show the dynamic variation of the duty ratio in steady state. There are slight variations in the duty ratio due to the real time estimation of the MPP. V_{DC}, i_{ma}, i_{mb} and i_{mc} are shown in Fig. 10. Moreover, Fig. 11 shows voltage across switch V_{sw}, current through the inductor i_L and the voltage across diode V_D. The time for the IGBT is on, the voltage across the IGBT is zero and a small fraction of voltage remains across the diode in this duration. Moreover, during this period, the inductor stores the energy and in the subsequent period, it releases the energy to the DC bus.

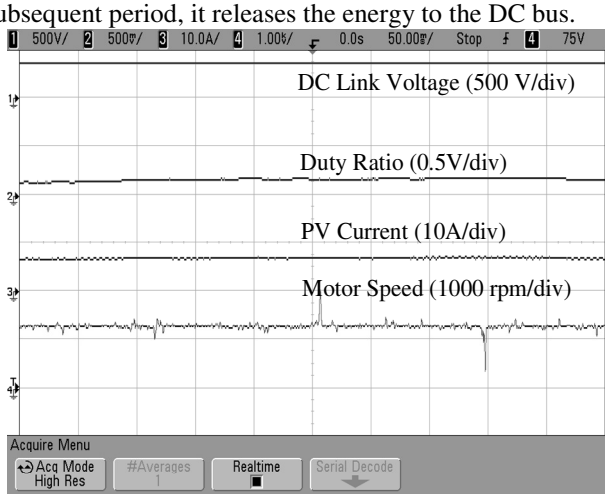

Fig. 9 Steady state characteristics of the system V_{DC}, D, I_{PV} and N_r

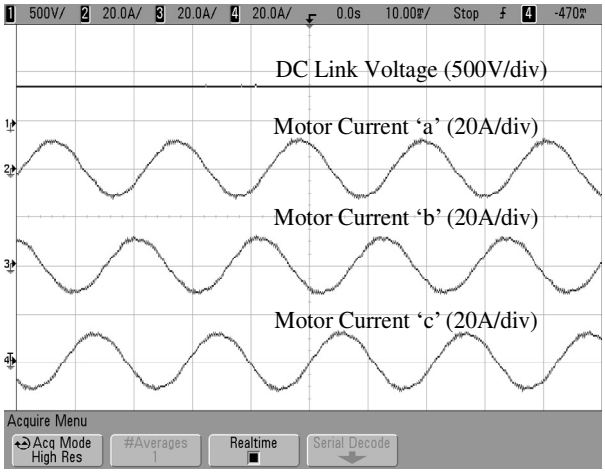

Fig. 10 Steady state characteristics of the system V_{DC}, i_{ma}, i_{mb} and i_{mc}

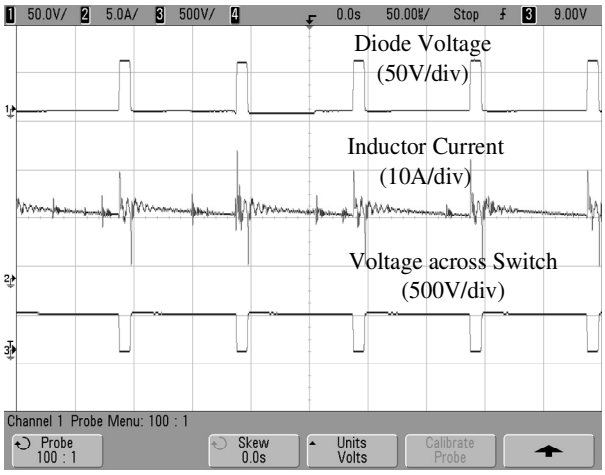

Fig. 11 Steady state characteristics of the system V_{SW}, i_L and V_D

This article has been accepted for publication in a future issue of this journal, but has not been fully edited. Content may change prior to final publication. Citation information: DOI 10.1109/TIA.2018.2825285, IEEE Transactions on Industry Applications

In Fig. 12, the torque generated T_e, duty ratio of the boost converter D, motor current i_{ma} and motor speed N_r are shown. Fig. 12 shows the mechanical parameters (torque, speed and power) in single scope and the fine perturbation in the duty ratio.

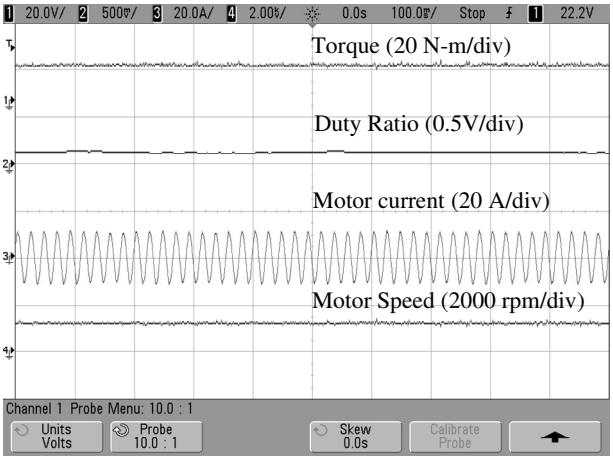

Fig. 12 Steady state characteristics of the system Te, D, i_{ma} and N_r

D. Dynamic Performance of Proposed System

The variation in the incident radiation is tested using PV simulator to show the satisfactory MPPT tracking. Initially the radiation has been at 1000 W/m^2, which is reduced to 500 W/m^2. Fig. 13 shows a variation in $V_{DC,}$ $I_{PV,}$ i_m and N_r. It can be deduced from the recorded waveforms that the DC link voltage is maintained constant and PV current is reduced to half. Fig. 14 shows the variation in the above mentioned parameters with an increase in the radiation from 500 W/m^2 to 1000 W/m^2.

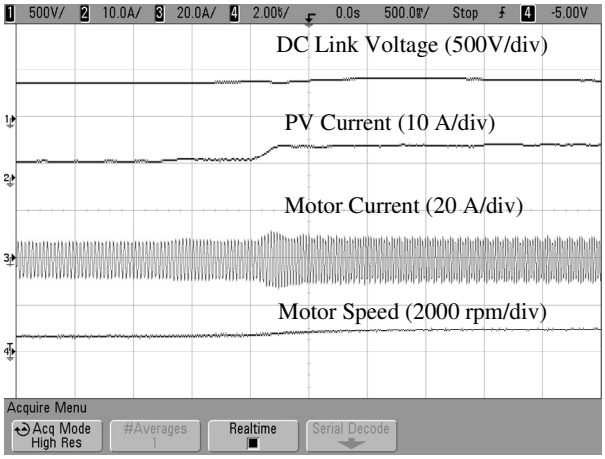

Fig. 13 Response under decrease in radiation from 1000 W/m^2 to 500 W/m^2

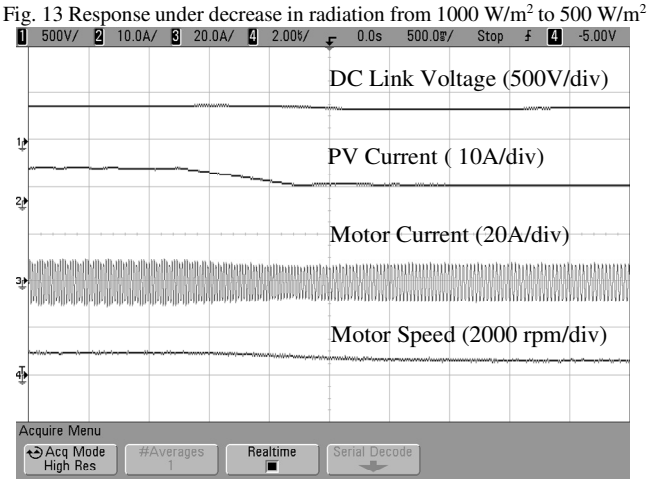

Fig. 14 Dynamic characteristics under decrease in radiation from 1000 W/m^2 to 500 W/m^2

VI. COMPARISION WITH SINGLE STAGE TOPOLOGY

The two stage system with DC bus clamping is studied along with the single stage with variable DC bus. The DC bus in the single state system is variable since it is tied to the PV array, hence with varying solar insolation, the PV array voltage reduces. A comparison of losses for a single stage and two stage systems, is given in Table II. It consists of developed AC voltage calculation at the terminals of the motor, and the line current is calculated considering the power factor of the induction motor as 0.8. The copper losses of an induction motor are calculated in both topologies with the calculated current. It is observed that the copper losses are always higher in the single stage system. It can be inferred from the calculation that as the radiation decreases the difference in the copper losses decreases because of the reduction in the current. Topology I refers to a single stage system while Topology II refers to a two stage system. Since the rated efficiency of the motor is 81% at rated voltage, the constant losses are calculated. These are considered to be constant throughout the operation.

$$\eta = 0.81 = \frac{P_{out}}{P_{in}} = \frac{P_{out}}{2200}$$

$$P_{out} = 1782 \text{ W}$$

$$P_{core\ loss} = P_{in} - P_{out} - P_{cu}$$

$$P_{core\ loss} = 2200 - 1782 - 3 \times 8.3^2 \times (0.603 + 0.7) = 148.7 \text{ W}$$

The motor current is calculated from the input power (Peak power available from PV array at any condition) as,

$$P_{in} = \sqrt{3} \times V_{ll} \times I_s \times pf \ .$$

VII. MAIN CONTRIBUTION OF PROPOSED CONTROL SCHEME

The proposed control system has salient feature of being immune to the variation in the estimation of the pump's constant. Moreover, the frictional loss across the pump column is well taken care off by the proposed control. A base speed/frequency reference is estimated from the MPPT algorithm, which depends on the pump's constant K_{pump}. However, an additional term is subtracted from this base speed/frequency, which is obtained from the PI controller. The error in DC bus voltage corresponds to the imbalance in the active power in the system and the losses of the converter. In the absence of the feed forward term, the estimated reference speed is generated by the PI controller. Hence, the performance is sluggish and dynamic behavior of the system is also not satisfactory. Moreover, even if wrong value of the pump's constant is chosen, the proposed control system estimates the reference speed accurately. Fig. 15 shows the performance of the proposed system with two pump's constants. One of these pump's constant deviates from the actual value. In the figure, the blue line corresponds to the control with the actual value of the pump's constant i.e. 6.554×10^{-4} Nm/rad^2/s^2. Moreover, the red curve depicts the performance when the pump constant is 8.025×10^{-4} Nm/rad^2/s^2. It is interesting to note that the output of the PI controller is about 4 rpm in the blue curve, while the same in the red curve is -88 rpm. The feed forward term or the base speed is 1372 rpm in blue curve while it reduces to 1286 rpm. This is because of an increase in the fed value of pump's constant. However, in both the cases, the subtraction of these quantities gives the accurate reference speed for the extraction of the maximum power from the PV array. The value of reference frequency is 45.8 Hz in both the cases.

This article has been accepted for publication in a future issue of this journal, but has not been fully edited. Content may change prior to final publication. Citation information: DOI 10.1109/TIA.2018.2825285, IEEE Transactions on Industry Applications

TABLE-II
COMPARISION OF THE COPPER LOSSES IN TWO DIFFERENT TOPOLOGIES

Radiation W/m^2/ PV Power	V_{mp} (V)	Max V_{ac} I (V)	Max V_{ac} II (V)	I_m I (A)	I_m II (A)	Stator Cu loss I	Stator Cu loss II	Slip power loss I	Slip power loss II	P_m(I) (W)/(η)	P_m(II) (W) /(η)
1000 (2.4 kW)	372.9	228.2	230	7.59	7.53	104.21	102.57	121	119.07	2023.09 (84.29)	**2029.66 (84.56)**
750 (1.8 kW)	368.8	225.7	230	5.75	5.64	59.81	57.54	69.43	66.80	1522 (84.55)	**1527 (84.83)**
500 (1.2 kW)	361.7	221.3	230	3.91	3.76	27.65	25.57	32.1	29.68	991.55 (82.62)	**996 (83)**
250 (0.6 kW)	347.1	212.4	230	2.03	1.88	7.45	6.39	8.65	7.42	435.2 (72.55)	**437.5 (73)**

Moreover, the DC bus voltage is settled to the reference value of 400 V. The proposed control algorithm, inherently is immune to the pump's constant.

Figs. 16 (a) and (b) show the overall cost effectiveness of the proposed system. The cost estimation is made from [24-25] in Indian Rupees. The analysis includes the bulk cost of major components. The total cost considering the major components comes out to be INR 6087 as shown in Fig. 16 (a). Moreover, a pie–chart illustrating the contribution of each component, is shown in Fig. 16 (b).

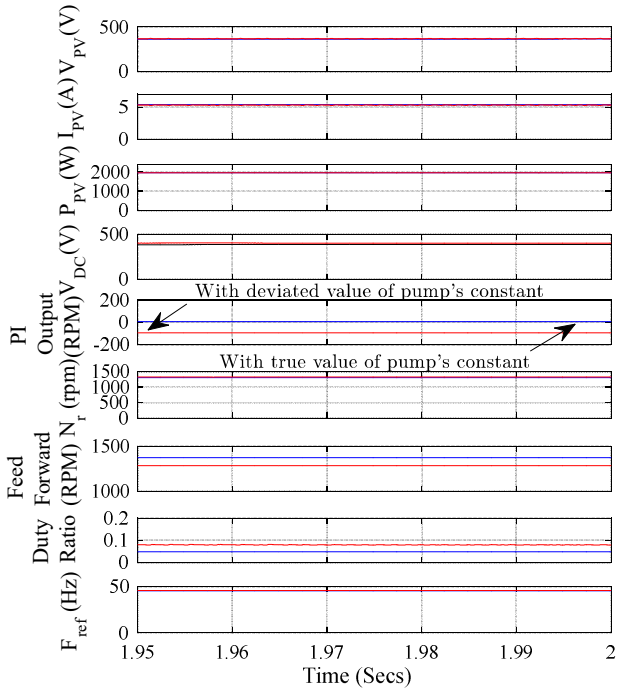

Fig. 15 Influence of the wrong estimation of pump's constant

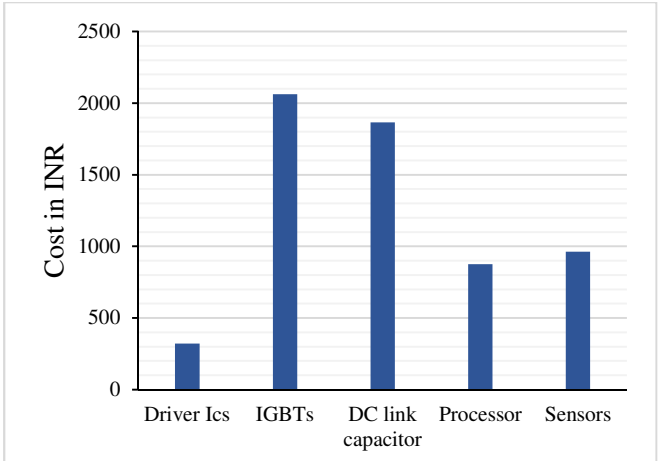

Fig. 16 (a) A brief cost estimation of the proposed solar water pumping system

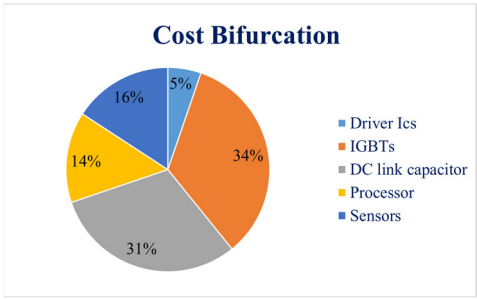

Fig. 16 (b) Cost bifurcation of the overall system

VIII. CONCLUSION

The standalone photovoltaic water pumping system with reduced sensor, has been proposed. It utilizes only three sensors. The reference speed generation for *V/f* control scheme has been proposed based on the available power the regulating the active power at DC bus. The PWM frequency and pump affinity law have been used to control the speed of an induction motor drive. Its feasibility of operation has been verified through simulation and experimental validation. Various performance conditions such as starting, variation in radiation and steady state have been experimentally verified and found to be satisfactory. The main contribution of the proposed control scheme is that it is inherently, immune to the error in estimation of pump's constant. The system tracks the MPP with acceptable tolerance even at varying radiation.

APPENDIX

Parameters of the proposed system: 2.2 kW(3HP), 230 V, 8.2 A, 50 Hz three phase, 1430 rpm, 4 pole, R_s = 0.603 Ω, R_r = 0.7 Ω, X_s = 1.007 Ω, X_r =0.9212 Ω, X_m = 23.56 Ω

REFERENCES

[1] E. Drury, T. Jenkin, D. Jordan, and R. Margolis, "Photovoltaic investment risk and uncertainty for residential customers," *IEEE J. Photovoltaics*, vol. 4, no. 1, pp. 278–284, Jan. 2014.

[2] E. Muljadi, "PV water pumping with a peak-power tracker using a simple six-step square-wave inverter," *IEEE Trans. on Ind. Appl.*, vol. 33, no. 3, pp. 714-721, May-Jun 1997.

[3] U. Sharma, S. Kumar and B. Singh, "Solar array fed water pumping system using induction motor drive," *1st IEEE Intern. Conf. on Power Electronics, Intelligent Control and Energy Systems (ICPEICES)*, Delhi, 2016.

[4] T. Franklin, J. Cerqueira and E. de Santana, "Fuzzy and PI controllers in pumping water system using photovoltaic electric generation," *IEEE Trans. Latin America*, vol. 12, no. 6, pp. 1049-1054, Sept. 2014.

[5] R. Kumar and B. Singh, "BLDC Motor-Driven Solar PV Array-Fed Water Pumping System Employing Zeta Converter," *IEEE Trans. Ind. Appl.*, vol. 52, no. 3, pp. 2315-2322, May-June 2016.

[6] S. Jain, A. K. Thopukara, R. Karampuri and V. T. Somasekhar, "A Single-Stage Photovoltaic System for a Dual-Inverter-Fed Open-End Winding Induction Motor Drive for Pumping Applications," *IEEE Trans. Power Elect.*, vol. 30, no. 9, pp. 4809-4818, Sept. 2015.

[7] J. Caracas, G. Farias, L.Teixeira and L. Ribeiro, "Implementation of a High-Efficiency, High-Lifetime, and Low-Cost Converter for an Autonomous Photovoltaic Water Pumping System," *IEEE Trans. Ind. Appl.*, vol. 50, no. 1, pp. 631-641, Jan.-Feb. 2014.

[8] R. Antonello, M. Carraro, A. Costabeber, F. Tinazzi and M. Zigliotto, "Energy-Efficient Autonomous Solar Water-Pumping System for Permanent-Magnet Synchronous Motors," *IEEE Trans. Ind. Electron.*, vol. 64, no. 1, pp. 43-51, Jan. 2017.
[9] M. Calavia1, J. M. Perié1, J. F. Sanz, and J. Sallán, "Comparison of MPPT strategies for solar modules," *in Proc. Int. Conf. Renewable Energies Power Quality, Granada,* Spain, Mar. 22–25, 2010.
[10] Trishan Esram and Patrick L. Chapman, "Comparison of photovoltaic array maximum power point tracking techniques," *IEEE Transactions on Energy Conversion EC*, vol. 22, no.2, pp. 439, 2007.
[11] Subudhi and R. Pradhan, "A comparative study on maximum power point tracking techniques for photovoltaic power systems," *IEEE Trans. Sustain. Energy*, vol. 4, no. 1, pp. 89–98, Jan. 2013.
[12] A. Garrigos, J. Blanes, J. Carrascoa, and J. Ejea, "Real time estimation of photovoltaic modules characteristics and its application to maximum power point operation*," Renew. Energy,* vol. 32, pp. 1059–1076, 2007.
[13] B. Singh, S. Kumar and C. Jain, "Damped-SOGI-Based Control Algorithm for Solar PV Power Generating System," *IEEE Trans. Ind. Appl.*, vol. 53, no. 3, pp. 1780-1788, May-June 2017.
[14] X. D. Sun, K. H. Koh, B. G. Yu and M. Matsui, "Fuzzy-Logic Based V/f Control of an Induction Motor for a DC Grid Power-Levelling System Using Flywheel Energy Storage Equipment," *IEEE Trans. Indus. Elect*., vol. 56, no. 8, pp. 3161-3168, Aug. 2009.
[15] S. R. Bhat, A. Pittet and B. S. Sonde, "Performance Optimization of Induction Motor-Pump System Using Photovoltaic Energy Source," *IEEE Trans. on Ind. App*., vol. IA-23, no. 6, pp. 995-1000, Nov. 1987.
[16] Y. Yao, P. Bustamante and R. Ramshaw, "Improvement of induction motor drive systems supplied by photovoltaic arrays with frequency control," *IEEE Trans. Energy Conv*., vol. 9, no. 2, pp. 256-262, Jun 1994.
[17] U. Sharma, B. Singh and S. Kumar, "Intelligent grid interfaced solar water pumping system," *IET Renewable Power Generation*, vol. 11, no. 5, pp. 614-624, March, 2017.
[18] Faramarz Karbakhsh, Mehdi Amiri and Hossein Abootorabi Zarchi, "Two-switch flyback inverter employing a current sensorless MPPT and scalar control for low cost solar powered pumps," *IET Renewable Power Generation*, vol. 11, no. 5, 2017
[19] S. Jain, R. Karampuri and V. Somasekhar, "An Integrated Control Algorithm for a Single-Stage PV Pumping System Using an Open-End Winding Induction Motor," *IEEE Trans. Ind. Elec.,* vol. 63, no. 2, pp. 956-965, Feb. 2016.
[20] A. Achour, D. Rekioua, A. Mohammedi, Z. Mokrani, T. Rekioua, S. Bacha, "Application of Direct Torque Control to a Photovoltaic Pumping System with Sliding-mode Control Optimization," *Electric Power Components and Systems*, vol. 44, no. 2, 2016.
[21] C. Slabbert and M. Malengret, "Grid connected/solar water pump for rural areas," *Proc. of . ISIE '98. IEEE International Symposium on Industrial Electronics*, Pretoria, 1998, pp. 31-34 vol.1.
[22] B. Singh, A. Chandra, and K. Al-Haddad, Power Quality: Problems and Mitigation Techniques. Chichester, U.K.: Wiley, 2015.
[23] N. Mohan, T. Undeland, and W. Robbins, "Power electronics: converters, applications and design", vol. 3, India John. Wiley & sons Inc., 2009.
[24] http://in.rsdelivers.com
[25] http://www.mouser.in

Bhim Singh (SM'99, F'10) was born in Rahamapur, Bijnor (UP), India, in 1956. He has received his B.E. (Electrical) from the University of Roorkee, India, in 1977 and his M.Tech. (Power Apparatus & Systems) and Ph.D. from the Indian Institute of Technology Delhi, India, in 1979 and 1983, respectively.

In 1983, he joined the Department of Electrical Engineering, University of Roorkee (Now IIT Roorkee), as a Lecturer. He became a Reader there in 1988. In December 1990, he joined the Department of Electrical Engineering, IIT Delhi, India, as an Assistant Professor, where he has become an Associate Professor in 1994 and a Professor in 1997. He has been ABB Chair Professor from September 2007 to September 2012. He has also been CEA Chair Professor from October 2012 to September 2017. He has been Head of the Department of Electrical Engineering at IIT Delhi from July 2014 to August 2016. Since, August 2016, he is the Dean, Academics at IIT Delhi. He is JC Bose Fellow of DST, Government of India since December 2015.

Prof. Singh has guided 69 Ph.D. dissertations, and 167 M.E./M.Tech./M.S.(R) theses. He has been filed 31 patents. He has executed more than eighty sponsored and consultancy projects. He has co-authored a text book on power quality: *Power Quality Problems and Mitigation Techniques* published by John Wiley & Sons Ltd. 2015.

His areas of interest include solar PV grid interface systems, microgrids, power quality monitoring and mitigation, solar PV water pumping systems, improved power quality AC-DC converters, power electronics, electrical machines, drives, flexible alternating transmission systems, and high voltage direct current systems.

Prof. Singh is a Fellow of the Indian National Academy of Engineering (FNAE), The Indian National Science Academy (FNA), The National Academy of Science, India (FNASc), The Indian Academy of Sciences, India (FASc), The World Academy of Sciences (FTWAS), Institute of Electrical and Electronics Engineers (FIEEE), the Institute of Engineering and Technology (FIET), Institution of Engineers (India) (FIE), and Institution of Electronics and Telecommunication Engineers (FIETE) and a Life Member of the Indian Society for Technical Education (ISTE), System Society of India (SSI), and National Institution of Quality and Reliability (NIQR).

He has received Khosla Research Prize of University of Roorkee in the year 1991. He is recipient of JC Bose and Bimal K Bose awards of The Institution of Electronics and Telecommunication Engineers (IETE) for his contribution in the field of Power Electronics. He is also a recipient of Maharashtra State National Award of Indian Society for Technical Education (ISTE) in recognition of his outstanding research work in the area of Power Quality. He has received PES Delhi Chapter Outstanding Engineer Award for the year 2006. Professor Singh has received Khosla National Research Award of IIT Roorkee in the year 2013. He is a recipient of Shri Om Prakash Bhasin Award-2014 in the field of Engineering including Energy & Aerospace. Professor Singh has received IEEE PES Nari Hingorani Custom Power Award-2017. He is also a recipient of "Faculty Research Award as a Most Outstanding Researcher" in the field of Engineering-2018 of Careers-360, India.

He has been the General Chair of the 2006 IEEE International Conference on Power Electronics, Drives and Energy Systems (PEDES'2006), General Co-Chair of the 2010 IEEE International Conference on Power Electronics, Drives and Energy Systems (PEDES'2010), General Co-Chair of the 2015 IEEE International Conference (INDICON'2015), General Co-Chair of 2016 IEEE International Conference (ICPS'2016) held in New Delhi, General Co-Chair of 2017 National Power Electronics Conference (NPEC) held in Pune.

Utkarsh Sharma (M'17) was born in Kota, India in 1991. He received B.Tech degree in electrical engineering from Sardar Vallabhbhai National Institute of Technology, Surat, India in 2013 and M.Tech degree in power electronics, electrical machines and drives (PEEMD) from the Indian Institute of Technology Delhi, India in 2016. Mr. Sharma is recipient of National Talent Search Scholarship (NTSE) awarded by National Council of Educational Research and Training (NCERT), New Delhi, India. Mr. Sharma received Best Industry Relevant M.Tech Thesis Award from Foundation for Innovation and Technology Transfer (FITT) at Indian Institute of Technology Delhi in 2016. He is currently working toward the Ph.D. degree in department of electrical engineering from the Indian Institute of Technology Delhi, New Delhi, India. His research interests include power electronics, control of electrical drives, renewable energy applications and design of special electrical machines.

Shailendra Kumar (S'15, M'17) was born in Mahoba, India, in 1988. He received B.Tech. degree in electrical and electronics enginnering from Uttar Pradesh Technical University, Lucknow, India, in 2010, and the M.Tech. degree in power electronics, electrical machine and drives (PEEMD) from the Indian Institute of Technology, Delhi, India, in 2015.

He is currently working toward the Ph.D. degree in department of electrical engineering from the Indian Institute of Technology Delhi, New Delhi, India. His research interests include power electronics, power quality, custom power devices and renewable energy. Mr. Kumar received the POSOCO power system award (PPSA) Award from Foundation for Innovation and Technology Transfer (FITT) at Indian Institute of Technology Delhi in 2016 and the IEEE UPCON Best Paper Award in 2016.